Plant Stress 17 (2025) 100958

Contents lists available at ScienceDirect

Plant Stress

journal homepage: www.sciencedirect.com/journal/plant-stress

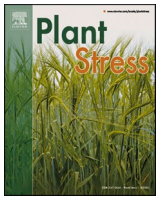

Acclimation of carbon metabolism to a changing environment across a leaf rosette of *Arabidopsis thaliana*

Vladimir Brodsky, Anian Kerscher [1], Michaela Urban [1], Thomas Nägele [*]

LMU München, Faculty of Biology, Plant Evolutionary Cell Biology, Großhaderner Str. 2-4, Planegg 82152, Germany

ARTICLE INFO

Keywords:
Arabidopsis thaliana
Cold acclimation
Leaf development
Photosynthesis
Carbon metabolism

ABSTRACT

Plants need to efficiently stabilize photosynthesis and carbon metabolism under changing environmental conditions to prevent irreversible tissue damage. For metabolic and biochemical analyses, leaves from different stages of *Arabidopsis thaliana* rosette development are frequently homogenized which might result in significant over- or underestimation of metabolite dynamics. In this study, photosynthesis and carbon metabolism were analyzed in mature and immature leaves of rosettes of natural *Arabidopsis* accessions originating from southern and northern Europe. The ambient growth condition at 22 °C was compared to a combined low temperature/elevated light treatment. Gradients of F_v/F_m and CO_2 assimilation rates across the leaf rosettes hinted towards tissue-specific acclimation capacities of photosynthesis and carbon metabolism. The dynamics of carbohydrates and carboxylic acids were integrated with photosynthetic parameters in a quantitative carbon balance model. Model simulations suggested that mature leaf tissue stabilizes acclimation of carbon metabolism in immature leaf tissue and other sink tissue. In conclusion, acclimation capacities of photosynthesis to low temperatures and elevated light significantly differ between leaves of one rosette. This directly affects carbon metabolism which shapes the metabolic acclimation capacity of the whole plant. It is discussed to consider such tissue-specific effects to support physiological interpretation of experimental data on photosynthetic and metabolic acclimation.

Introduction

Plant metabolism is highly plastic and allows for efficient buffering of environmental dynamics (Shaar-Moshe et al., 2019). Central to environmentally induced metabolic adjustments is the balance of primary and secondary photosynthetic reactions, i.e., balancing of photosynthetic light energy absorption and biochemical carbon fixation within the Calvin-Benson-Bassham cycle (CBBc). Carbohydrates are the direct products of photosynthetic CO_2 fixation, and regulation of their metabolism plays a central role in plant acclimation to environmental changes (Rolland et al., 2006; Ruan et al., 2010). In photosynthetically active leaf tissue, triose phosphates are synthesized in the CBBc and provide carbon equivalents for biosynthesis of transitory starch and sucrose. In a changing light and/or temperature regime, the balance of carbon fluxes towards storage compounds, e.g., starch, and soluble sugars was found to be of central importance for the acclimation capacity. For example, enzymatic deficiency in the starch degradation pathway was reported to result in impaired freezing tolerance which was accompanied by a significantly affected metabolism and accumulation response of soluble sugars (Yano et al., 2005). Similarly, starch deficiency resulted in a delay of hexose accumulation during cold exposure which suggested a role of starch degradation in augmentation of soluble sugars during early cold response (Sicher, 2011). Particularly, during the early period of cold exposure, such augmentation might be essential to sustain energy metabolism until adjustments in transcription, translation and metabolic regulation have stabilized metabolism.

Sucrose biosynthesis, catalysed by sucrose phosphate synthase (SPS) enzymes, has been shown earlier to make an essential contribution to photosynthetic cold acclimation (Strand et al., 2003; Nägele et al., 2012). Fructose 6-phosphate and UDP-glucose are substrates for the SPS reaction which yields sucrose 6-phosphate being immediately dephosphorylated by sucrose phosphate phosphatase (SPP). Sucrose might serve as a substrate for carbon export into sink organs or can be hydrolyzed by invertase enzymes which are located in different compartments, e.g., the cytosol and vacuole (Sturm, 1999; Roitsch and González, 2004; Nägele, 2022). Glucose and fructose, which are products of invertase reactions, are substrates for hexokinases which, in an ATP-dependent manner, phosphorylate both hexoses to produce glucose

* Corresponding author.
E-mail address: thomas.naegele@lmu.de (T. Nägele).
[1] These authors contributed equally to this work.

https://doi.org/10.1016/j.stress.2025.100958
Received 6 May 2025; Received in revised form 15 July 2025; Accepted 16 July 2025
Available online 17 July 2025

6-phosphate (G6P) and fructose 6-phosphate (F6P), respectively (Granot et al., 2013). As G6P is substrate for UDP-glucose biosynthesis, these reactions constitute a potential cycle of sucrose cleavage and re-synthesis which has been discussed before to be involved in carbon partitioning and stabilization of carbohydrate metabolism against environmental perturbation (Geigenberger and Stitt, 1991; Fürtauer and Nägele, 2016).

Carbohydrates are well known to be essential in metabolic and photosynthetic regulation in a changing environment. Yet, physiological interpretation of carbohydrate dynamics is frequently challenging due to their multiple roles in metabolism, signaling and development (Moore et al., 2003; Ruan, 2014). For example, due to being a substrate for hydrolysis and carbon export from source to sink tissue, sucrose dynamics might be explained in different ways: either due to a changed balance between biosynthesis and hydrolysis, or between biosynthesis and export rates. Further, sink-source relationships between plant tissues change in the life cycle of a plant which simultaneously affects expression and activity patterns of enzymes and transporters involved in sugar metabolism (Koch, 2004; Durand et al., 2018). For example, the switch from juvenile to adult phases is accompanied by sugar-induced repression of microRNA156 (miR156) which results in a promotion of expression of adult traits (Yu et al., 2013). Also, the transition to flowering has been found to be related to sugar metabolism and transport in many species (Bernier et al., 1993). Here, the sucrose facilitator SWEET10 represents a downstream element of FLOWERING LOCUS T (FT) which is a positive regulator of flowering (Andrés et al., 2020). FT was observed to induce expression of SWEET10 in leaf veins and the shoot apex, and to accelerate flowering (Andrés et al., 2020).

Cyclic interconversion of metabolites, such as sucrose, makes analysis of observed carbohydrate dynamics non-intuitive due to an increased number of explanatory models of metabolism. To support the analysis and interpretation, mathematical modelling of metabolite dynamics has been proven useful in previous studies (Stelling et al., 2002; Shi and Schwender, 2016; Töpfer et al., 2020). Frequently, ordinary differential equation (ODE) systems are applied for kinetic modelling and simulation of metabolite dynamics over time. In such a model, ODEs are used to describe metabolite dynamics by the sum of in- and output fluxes which might comprise biosynthesis, interconversion or transport processes. In a kinetic model, these processes are typically described by enzyme kinetic terms which contain experimentally determined enzyme parameters and variables, e.g., values of K_M, K_i and v_{max}. Finally, model simulation, i.e., numerical integration of the ODE system, results in metabolite concentrations which can be evaluated experimentally.

In the present study, we have combined experimental analysis of photosynthesis and carbohydrate metabolism with kinetic modelling. Our aim was to reveal effects of cold and elevated light on metabolic regulation across old (mature) and young (immature) leaf tissue in natural accessions of *Arabidopsis thaliana*. The accessions originated from northern and southern Europe reflecting a broad geographical range of European *Arabidopsis* populations. Based on an observed significant gradient of maximum quantum yield of photosystem II between old and young leaves under low temperature and elevated light, it was hypothesized that this was also reflected in carbon metabolism. Differential dynamics of carbohydrates and carboxylic acids further supported a tissue-specific photosynthetic and metabolic acclimation process.

Materials and methods

Plant material and growth conditions

Natural accessions of *Arabidopsis thaliana*, Ct-1 (geographical origin: Catania, Italy; NASC ID: N6674), Fei-0 (geographical origin: St. Maria d. Feiria, Portugal; NASC ID: N22645), Oy-0 (geographical origin: Oystese, Norway; NASC ID: N6824) and Rsch-4 (geographical origin: Rschew/Starize, Russia; NASC ID: N6850), were grown on a 1:1 mixture of GS90 soil and vermiculite in a climate chamber under controlled short-day conditions (8 h/16 h light/dark; 100 µmol m^{-2} s^{-1}; 22 °C/16 °C; 50–60 % relative air humidity). After eight weeks, plants were sampled at the end of night (eon), and at the end of day (eod). For treatment, plants were transferred to a cold room for low temperature and elevated light treatment (LT/EL; 8 h/16 h light/ dark; 250 µmol m^{-2} s^{-1}; 4–6 °C/4 °C, 40–50 % relative air humidity). This combined treatment was chosen because it represents a naturally occurring environment which might challenge populations of *Arabidopsis* in their natural habitats (Rasmussen et al., 2013). After 7 days at LT/EL, plants were sampled at eon and eod. Young and old/mature leaves were cut at the petiole with a scalpel within the growth cabinets, immediately quenched in liquid nitrogen and stored for up to three months at −60 °C until further use. Leaves which constituted the first rosette were classified as 'old/-mature'. All tissue above was classified as 'young'. A schematic overview of sampled young/old tissue is provided in the supplements (Supplementary Fig. S1).

Net photosynthesis and chlorophyll fluorescence measurements

Net rates of CO_2 assimilation (*Net PhotoSynthesis*, NPS) were recorded at 100 µmol m^{-2} s^{-1} for control plants and 250 µmol m^{-2} s^{-1} for LT/EL plants, respectively. Measurements were conducted after three to four hours in the light period (i.e., around midday), with a WALZ GFS-3000FL system (Heinz Walz GmbH; www.walz.com). Due to the need of a leaf length of at least 3–4 cm to fit into the measurement cuvette, the youngest leaves of rosettes were not included in the gas exchange measurements.

Parameters of chlorophyll fluorescence were obtained through Imaging-PAM MAXI version at ambient temperature (Heinz Walz GmbH; www.walz.com). Maximum quantum yield of PSII (F_v/F_m) was determined after 15 min of dark adaptation of the rosette and subsequently supplying a saturating light pulse.

All photosynthetic measurements were conducted at 22 °C and repeated on three independent samples, i.e., leaf rosettes. Young leaves which were measured did not comprise the smallest/youngest leaves.

Quantification of starch and soluble carbohydrates

Transitory starch and soluble carbohydrate amounts were determined as described before (Kitashova et al., 2023). Fresh leaves mixed with sea sand were homogenized in 80 % ethanol and incubated at 80 °C for 30 min. The supernatant, containing the soluble sugars, was separated from the starch-containing pellet and transferred to a separate tube for further analysis. Pellets were hydrolyzed in 0.5 N NaOH at 95 °C for 60 min and acidified with 1 M CH_3COOH. The suspension was then subjected to amyloglucosidase digestion. Resulting glucose moieties were quantified photometrically at 540 nm in a coupled glucose-oxidase/peroxidase/dianisidine assay.

Ethanol of previously obtained soluble sugar fractions was evaporated and the dried residue solubilized in water. Sucrose was quantified by incubating the samples in 30 % KOH at 95 °C for 10 min before adding 0.14 % (w/v) anthrone in 14.6 M H_2SO_4 and incubating at 40 °C for 30 min. Complexes were photometrically detected and quantified with a calibration curve at 620 nm.

Glucose amounts were obtained in a coupled enzymatic assay of hexokinase and glucose-6-phosphate dehydrogenase (G6PDH), while fructose amounts were quantified via a coupled hexokinase/phosphoglucose isomerase/G6PDH assay. In both cases, $NADP^+$ was reduced to yield $NADPH+H^+$ which was quantified at 340 nm.

Starch and soluble carbohydrates were determined in five independent replicates.

Quantification of enzyme activities

Enzyme activities under optimal temperature and substrate saturation (v_{max}) were obtained for sucrose phosphate synthase (SPS),

glucokinase (GLCK), fructokinase (FRCK), and invertase (INV) as described previously (Kitashova et al., 2023).

Leaf tissue was homogenized with sea sand in 50 mM HEPES pH 7.5, 10 mM $MgCl_2$, 1 mM EDTA, 2.5 mM DTT, 10 % (v/v) glycerine and 0.1 % (v/v) Triton X-100. SPS enzymes were extracted on ice for 20 min. Following centrifugation at 4 °C with 20,000 g, the supernatant was incubated for 30 min at 25 °C with 50 mM HEPES pH 7.5, 15 mM $MgCl_2$, 2.5 mM DTT, 35 mM UDP-glucose, 35 mM F6P and 140 mM G6P. The activity assay was stopped by boiling samples with 30 % KOH and sucrose amounts were determined with an anthrone assay as described above.

For glucokinase (GLCK) and fructokinase (FRCK) enzyme activity assays, homogenized leaf tissue was extracted in 50 mM Tris pH 8.0, 0.5 mM $MgCl_2$, 1 mM EDTA, 1 mM DTT and 1 % (v/v) Triton X-100. Samples were centrifuged at 4 °C with 20,000 g and the supernatant was combined with a buffer containing 100 mM HEPES pH 7.5, 10 mM $MgCl_2$, 2 mM ATP, 1 mM $NADP^+$, 0.5 U G6PDH. Activities were determined from changes of $NADPH+H^+$ over time after addition of 5 mM glucose or fructose, for respective measurements of $v_{max:GLCK}$ and $v_{max:FRCK}$, at 30 °C and 340 nm.

Cytosolic (nINV) and vacuolar (aINV) invertase activities were determined in 50 mM HEPES–KOH pH 7.5, 5 mM $MgCl_2$, 2 mM EDTA, 1 mM phenylmethylsulfonylfluoride, 1 mM DTT, 10 % (v/v) glycerol and 0.1 % (v/v) Triton X-100 on ice. The suspension was centrifuged at 4 °C with 20,000 g incubated in (I) a nInv-specific reaction buffer with a pH of 7.5, containing 20 mM HEPES–KOH and 100 mM sucrose, or (II) an aInv-specific reaction buffer at pH 4.7, containing 20 mM sodium acetate and 100 mM sucrose. After incubation at 30 °C, the reactions were stopped at 95 °C. Glucose was determined photometrically at 540 nm by a coupled glucose oxidase/peroxidase/dianisidine assay.

All enzyme activities were determined in three to four independent replicates.

Quantification of carboxylic acids

Absolute amounts of citrate, fumarate and malate were determined using photometric assay kits (Sigma-Aldrich, MAK057, MAK060 and MAK067, www.sigmaaldrich.com). For extraction, leaf tissue was ground to a fine powder in liquid nitrogen before double distilled water of 60 °C was added, and the sample was immediately incubated at 95 °C for 15 min. After brief centrifugation, the supernatant was used for photometric measurements. Amounts of carboxylic acids were determined in three independent replicates.

Data evaluation and mathematical modelling

Data was statistically analyzed in R Version 3.6.2 (www.r-project.org; R Core Team 2019) and RStudio Version 1.2.5033 (www.rstudio.com; RStudio Team 2019). Significances of NPS and F_v/F_m were evaluated using a two-way ANOVA model with variables of growth condition and tissue age. Metabolite amounts and enzyme activities were analyzed with a three-way ANOVA model with variables of growth condition, tissue age and sampling timepoint. Mathematical modelling was performed in MATLAB Version 24.2.0.2740171 (R2024b) (www.mathworks.com) with the IQM Tools Toolbox, developed by IntiQuan (www.intiquan.com) and the curve fitting toolbox. All data on metabolite amounts, enzyme activities, and NPS rates is provided in the supplements (Supplementary Table ST1).

For parameter estimation, a particle swarm pattern search method for bound constrained global optimization was utilized (Vaz and Vicente, 2007). A cost function was minimized which quantified squared errors between simulations and experimental data.

The model described a simplified approximation of the central leaf carbohydrate metabolism of *Arabidopsis thaliana*. It was assumed that carbon equivalents can be exchanged between young and old leaves (Fig. 1). To simulate the metabolic environment, a set of ordinary differential equations was used to describe daily dynamics of metabolite concentrations. Experimentally determined enzyme activities were used to simulate Michaelis-Menten kinetics with parameters K_i and K_m derived from a previous study (Nägele et al., 2010). All models are provided in the supplements (Supplementary Data F1).

In simulations of metabolism under low temperature, enzymatic rates were adjusted to the temperature regime by multiplication with the correction factor T_{Arrh}, which was selected from the interval $I_{temp} = [0.25; 0.4]$. This factor was described previously as the reduction of maximal enzymatic activity resulting from thermodynamic constraints acting on the enzyme at 4 °C. It was obtained by logarithmic conversion of the Arrhenius equation and providing the desired experimental temperature (Kitashova et al., 2023).

The system input function was described by NPS carbon assimilation rates. For control plants, measured values were used in the model because the growth conditions reflected the measurement temperature (22 °C). For LT/EL plants, NPS rates were also determined at 22 °C and, for modelling, corrected by a factor between 0.6 - 0.8 which was based

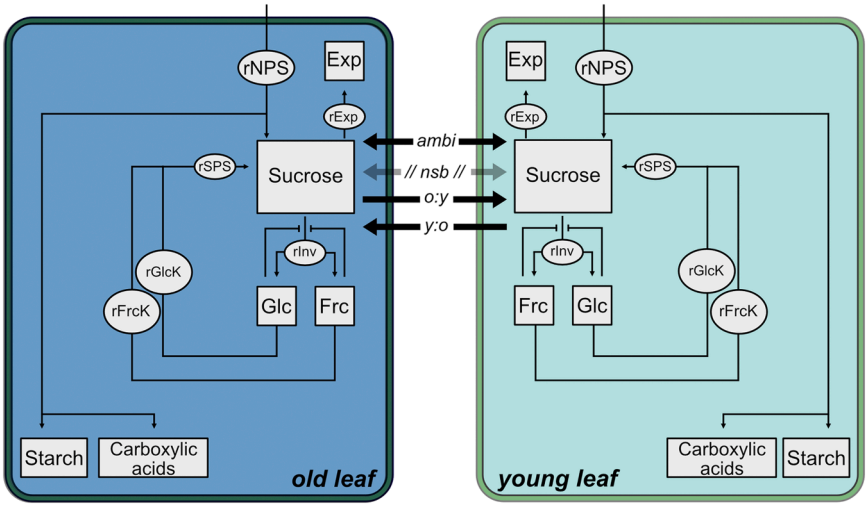

Fig. 1. Model of putative metabolic interactions between carbon metabolism in young and old leaf tissue. rExp: (unspecific) sucrose transport to other sinks (tissues and pathways); Glc: glucose; Frc: fructose; rNPS, rate of net photosynthesis; rSPS, rate of sucrose phosphate synthase; rInv, rate of invertase; rGlck, rate of glucokinase; rFrck, rate of fructokinase; *ambi*: ambidirectional sucrose transport; *nsb*: no sucrose transport between tissues; *o:y*: sucrose transport from old to young tissue; *y:o*: sucrose transport from young to old tissue. Arrows with blunt ends indicate feedback inhibition by products, i.e., feedback inhibition of invertases by hexoses.

on previous measurements of NPS at 4 °C (Nägele et al., 2011; Nägele and Heyer, 2013; Kitashova et al., 2023). The corrected values of NPS were also used for correlation analysis. From these rates, transitory starch and the dynamics of summed carboxylic acids (i.e., citrate, fumarate, malate) were subtracted. This metric was quantified by adding the median of diurnal starch accumulation to the mean of carboxylic acid accumulation and calculating the hourly accumulation rate assuming a linear rate across the light phase, i.e., 8 h. This value was subtracted from the mean value of the carbon assimilation rate and stoichiometrically adjusted to represent the rate of carbon-input in C_6 units. Calculated uptake rates were compared to the maximal activity of SPS enzymes. Due to the finding that the sucrose input was verified to be lower than the SPS v_{max} under all conditions, these model assumptions were maintained.

For carbohydrate and enzyme data, parameter bounds were set to the 25th and 75th quartiles derived from the experimental data. In the case of invertase activity, v_{max} of acidic and neutral invertases were summarized and parametric bounds were constrained to the range from lower to upper standard deviation from the mean.

Maximal bounds for a putative export of sucrose were set empirically for each accession x condition. Models that did not contain a sucrose bridging point between old and young leaves (nsb) had their upper bound of sucrose export (*k_exp*) adjusted in integer steps until a solution was found that could explain experimentally determined data. This *k_exp* was then fixed for the other models of the same accession x condition and the bounds for export of sucrose into the other leaf were kept as the same as the ones for *k_exp*. In general, the unspecific export of sucrose (*rExp*) might represent any tissue and/or metabolic pathway.

Results

Photosynthesis is affected by leaf development

The analysis of maximum quantum yield of photosystem II (F_v/F_m) revealed a significant developmental effect of leaf tissue during cold acclimation across all tested natural accessions Ct-1, Fei-0, Oy-0 and Rsch-4 (Fig. 2). Generally, F_v/F_m values did not differ significantly between leaf tissues under ambient temperature. Yet, upon exposure to LT/EL, F_v/F_m values of old leaves were observed to be significantly lower than in young tissue (ANOVA, $p < 0.05$).

To evaluate if these differences were related to carbon assimilation, rates of net photosynthesis (NPS) were quantified. All NPS rates were quantified at 22 °C applying the respective growth PAR intensities, i.e., 100 µmol photons m^{-2} s^{-1} for control plants and 250 µmol photons m^{-2} s^{-1} for LT/EL plants. At 22 °C, young leaves had a lower NPS than old leaves, except for Fei-0 where no difference was detected between both tissues (Fig. 3; ANOVA, $p < 0.05$). Consistently across all accessions, under LT/EL, mean rates of NPS in young leaves were found to be higher than in old leaves while this effect was only found to be significant in Ct-1 (Fig. 3A; ANOVA, $p < 0.05$). Due to the constant temperature regime at which NPS was quantified for both control and LT/EL plants, a direct comparison between both conditions was not possible. However, this measurement setup (instead of adjusting the temperature to 4 °C for LT/EL plants) was chosen to reveal cold-induced regulatory response in old and young tissue, respectively.

Comparing both F_v/F_m and NPS in a principal component analysis (PCA) revealed a separation of both growth regimes along principal component (PC) 1, capturing 65.1 % of the total variance (Fig. 4). The separation was more pronounced for young than for old tissue. Both tissue types were separated along PC2 which captured ~36 % of total variance. The (approximately) perpendicular orientation of both loadings, i.e., F_v/F_m and NPS, revealed that they were not correlated.

Leaf development affects dynamics of central pools of carbon metabolism

Sucrose and transitory starch are central products of photosynthetic CO_2 fixation and represent an essential branching point for carbon allocation within leaf metabolism. Consistently, across accessions, tissue types and conditions, both carbohydrates were observed to increase during the light phase (Fig. 5). In all accessions, starch accumulated significantly during the day at 22 °C in both old and young leaf tissue (Fig. 5A-D). At LT/EL, the accessions differed in their starch accumulation pattern: Ct-1 showed a significant starch accumulation only in young tissue (Fig. 5A), while no diurnal accumulation was observed in Fei-0 anymore (Fig. 5B). In Oy-0 and Rsch-4, both young and old tissue showed a significant starch accumulation (Fig. 5C, D).

Under ambient conditions, sucrose amounts were found to be similar across accessions and leaf tissues (Fig. 5E-H). At LT/EL, sucrose amounts were observed to be elevated in all leaf tissues of all accessions. Further, diurnal sucrose accumulation was pronounced under LT/EL and resulted in highest levels in young leaf tissue.

Under ambient conditions, the amounts of free hexoses glucose and

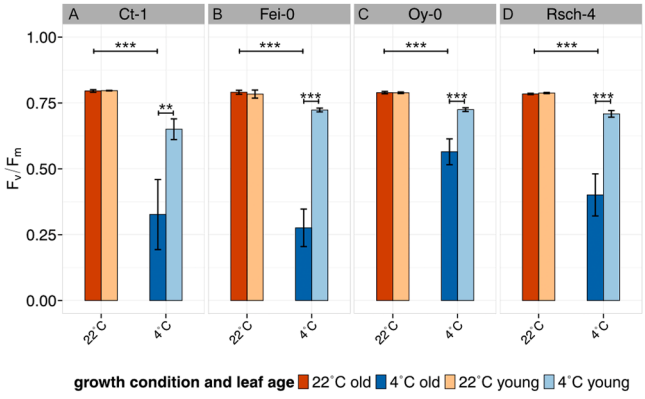

Fig. 2. Maximum quantum yield of photosystem II (F_v/F_m) at low temperature and elevated light. (A) Ct-1, (B) Fei-0, (C) Oy-0, (D) Rsch-4. Bars represent means ± SD, $n = 3$. Orange: ambient temperature conditions, blue: 7d of LT/EL. Light shade: young leaves, dark shade: old leaves. Asterisks indicate significance (ANOVA + Tukey HSD post hoc test; ** $p < 0.01$; *** $p < 0.001$). A full table of ANOVA results is provided in the supplements (Supplementary Table ST2).

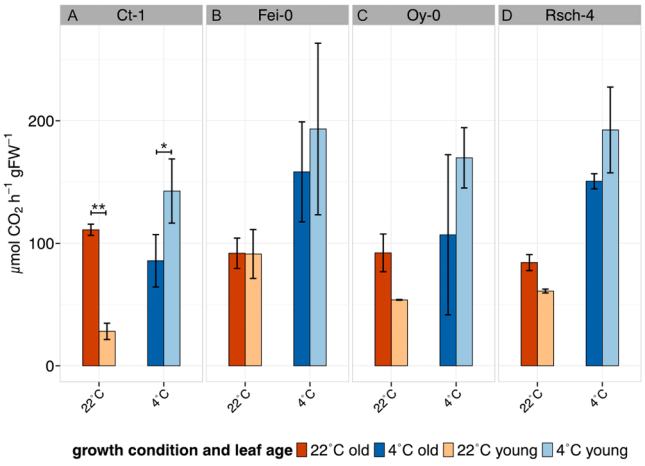

Fig. 3. Rates of net carbon assimilation across all tested accessions, tissues and growth conditions. (A) Ct-1, (B) Fei-0, (C) Oy-0, (D) Rsch-4. All rates were determined at 22 °C and growth PAR intensity, i.e., at 100 µmol photons m^{-2} s^{-1} for control plants and at 250 µmol photons m^{-2} s^{-1} for LT/EL plants. Bars represent means ± SD, $n = 3$. Orange: ambient temperature conditions, blue: 7d of LT/EL. Dark shade: old leaves; Light shade: young leaves. Asterisks indicate significance (ANOVA + Tukey HSD post hoc test; * $p < 0.05$; ** $p < 0.01$). A full table of ANOVA results is provided in the supplements (Supplementary Table ST2).

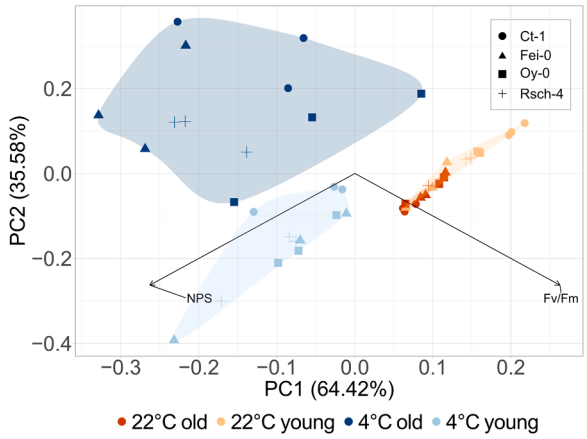

Fig. 4. Principal component analysis of F_v/F_m and rates of NPS across accessions, growth conditions and leaf tissues. Parameters were determined at 22 °C and growth PAR intensity, i.e., at 100 µmol photons m^{-2} s^{-1} for control plants and at 250 µmol photons m^{-2} s^{-1} for LT/EL plants. Orange: ambient temperature conditions, blue: 7d of LT/EL. Light shade: young leaves, dark shade: old leaves. Shapes indicate accessions: Ct-1: circles; Fei-0: triangles; Oy-0: squares; Rsch-4: crosses.

fructose showed slight dynamics during the day which was, however, different between accessions (Fig. 6). While Ct-1 showed constant glucose amounts, Fei-0 and Oy-0 were found to increase their glucose amounts until end of the day (Fig. 6A–C). More consistently, under LT/EL, the amounts of both hexoses increased in all accessions. Under these conditions, in Fei-0 and Oy-0, glucose was found to accumulate significantly during the light phase, particularly in young tissue, whereas fructose amounts remained constant (Fig. 6E-H).

To reveal whether exposure to LT/EL affected metabolism of carboxylic acids, amounts of citrate, fumarate and malate were quantified (Fig. 7, Supplementary Figures S2-S4). At 22 °C, the amounts of carboxylic acid in old leaves were approximately twice as high as in young leaves. Exposure to LT/EL resulted in a similar total amount of carboxylic acids in young and old leaves. Only in Fei-0, amounts in young leaves under LT/EL were lower than in old leaves (Fig. 7B).

Carbon balance relates differently to metabolism in young and old leaf tissue

Net carbon fluxes during the light phase were estimated by balancing carbon uptake rates (NPS), carbon turnover (C(to)) and carbon export to other tissue and/or pathways (EXP). C(to) was calculated by stoichiometrically converting metabolite pools to C6 equivalents and assessing their (summed) accumulation rates per hour during the 8-hour light phase. EXP was then derived as the difference between NPS and C(to). These estimated export rates thus comprised all carbon which was not reflected in dynamics of quantified carbohydrates and carboxylic acids. Potentially, this also comprised carbon exported to (other) sink tissue like roots or meristems which were not contained in the analysed samples. A Pearson correlation analysis revealed that young and old tissue showed a different relation between metabolites and enzymes to these estimated carbon fluxes under environmental changes which suggested differential regulation of metabolism and photosynthesis (Fig. 8, Supplementary Fig. S5).

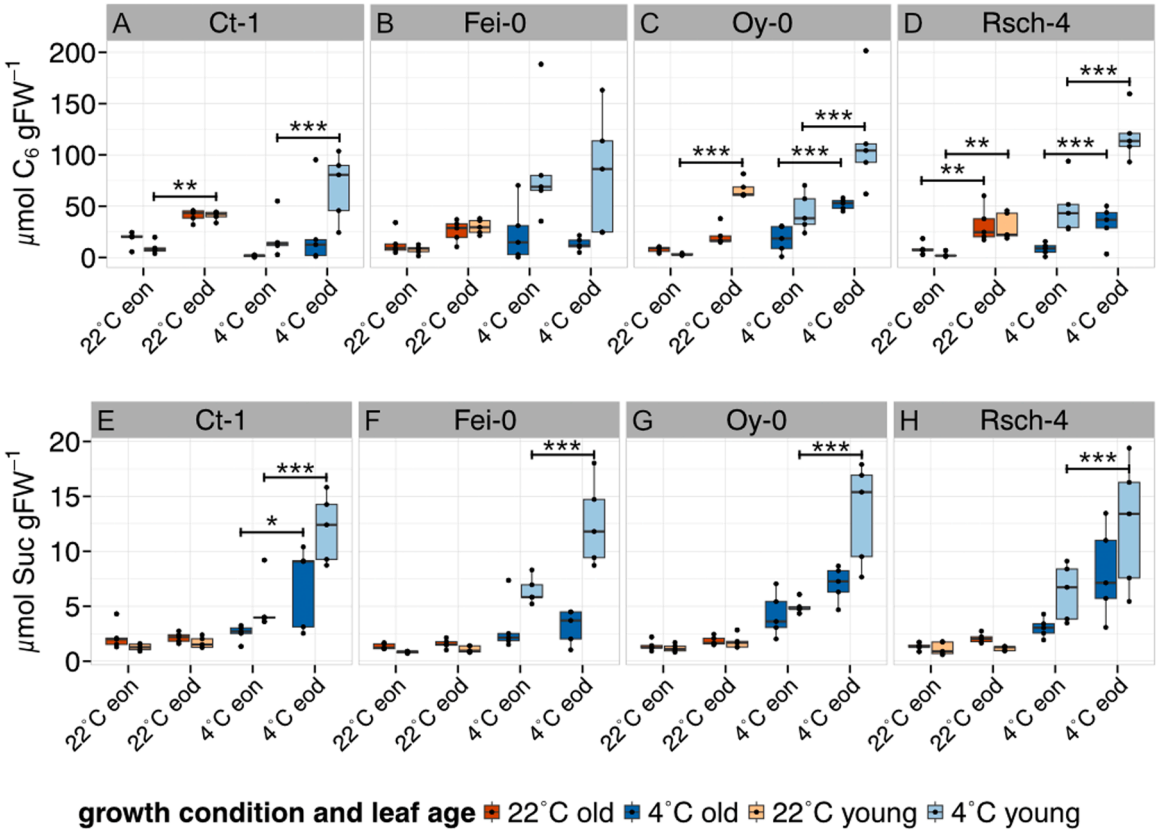

Fig. 5. Diurnal dynamics of starch and sucrose amounts. (A) – (D) Diurnal dynamics of starch amounts, expressed as C_6 moieties, in old and young tissue of natural accessions before (22C) and after (4C) LT/EL treatment. (E) - (H) Diurnal dynamics of sucrose amounts in old and young tissue of natural accessions before (22C) and after (4C) LT/EL treatment. Orange: ambient temperature conditions, blue: 7d of LT/EL. Light shade: young leaves, dark shade: old leaves. n = 5. Asterisks indicate significance (ANOVA + Tukey HSD post hoc test; * $p < 0.05$; ** $p < 0.01$; *** $p < 0.001$). Significance is shown only for diurnal dynamics within accession, tissue and condition. A full table of ANOVA results is available in the supplements (Supplementary Table ST3).

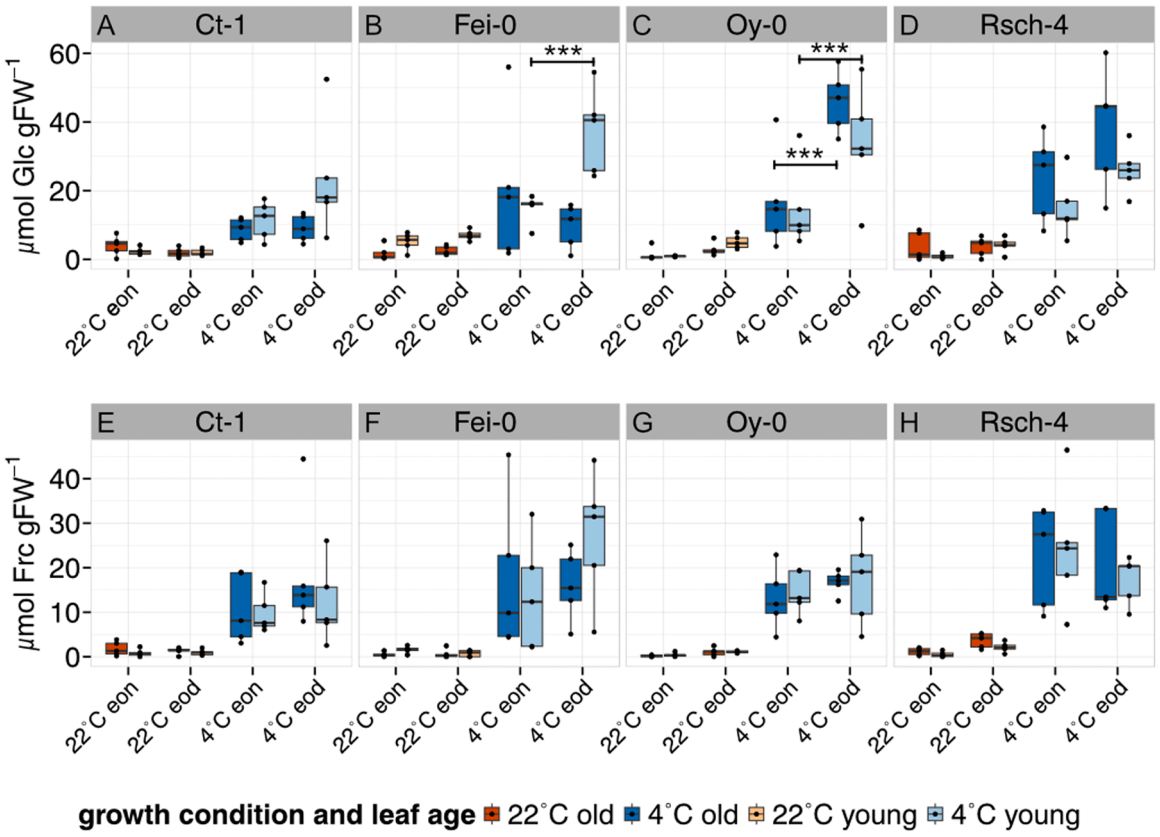

Fig. 6. Dynamics of glucose and fructose amounts. (A) - (D) Diurnal dynamics of glucose in old and young tissue of natural accessions before (22C) and after (4C) LT/EL treatment. (E) - (H) Diurnal dynamics of fructose in old and young tissue of natural accessions before (22C) and after (4C) LT/EL treatment. Orange: ambient temperature conditions, blue: 7d of LT/EL. Light shade: young leaves, dark shade: old leaves. n = 5. Asterisks indicate significance (ANOVA + Tukey HSD post hoc test; *** $p < 0.001$). Significance is shown only for diurnal dynamics within accession, tissue and condition. A full table of ANOVA results is available in the supplements (Supplementary Table ST3).

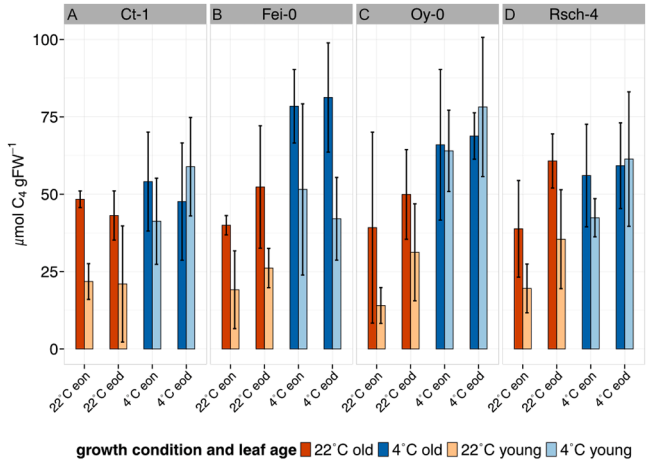

Fig. 7. Diurnal dynamics of carboxylic acids. Summed quantities (in C4 units) of citrate, fumarate and malate for (A) Ct-1, (B) Fei-0, (C) Oy-0, (D) Rsch-4. Bars represent means ± SD, $n = 3$. Orange: ambient temperature conditions, blue: 7d of LT/EL. Light shade: young leaves, dark shade: old leaves. A summary of each carboxylic acid is provided in the supplements (Supplementary Figs. S2–S4).

Both young and old leaf tissue showed a significantly negative correlation between EXP and C(to), but this correlation was much stronger in old leaf tissue (Fig. 8B, C). In contrast, only in young leaf tissue, rates of NPS correlated positively with soluble carbohydrates and carboxylic acids while no significant correlation was observed in old leaf tissue. Further, sucrose and SPS activity were both negatively correlated with EXP only in old leaf tissue, while in young tissue no significant correlation was observed. This indicated a differential metabolic regulation of the total carbon balance in both types of tissue.

As these observations hinted towards a differential metabolic regulation of carbon uptake and release in young and old leaf tissue, a metabolic model was developed based on ordinary differential equations. The model described dynamics of sucrose turnover, carbon uptake, and export during the 8 h light phase. To test whether the kinetic model could indicate a putative interaction of carbon metabolism in young and old leaf tissue, four flux scenarios were tested to account for potential sucrose exchange between young and old leaves. In the first scenario, both young and old metabolism was simulated independently describing the carbon balance equation as a non-specific export (*nsb*). In two further models, a directional flux from young to old (*y:o* model), or from old to young (*o:y* model) leaf tissue was implemented. Finally, in a fourth simulation scenario, a bidirectional exchange of sucrose between young and old tissue was assumed (*ambi* model). Model performance was assessed by the optimized cost function which represented least square errors between simulated and experimentally measured metabolite concentrations, i.e., the lower the cost function the better the fit of experimental data was.

Simulation of metabolism in Ct-1 and Oy-0 at 22 °C revealed best fits for *ambi* and *o:y* models (Fig. 9A, C). In Fei-0, simulations with lowest cost functions were realized by *ambi* and y:o models (Fig. 9B) while similar solution quality across all models was found for Rsch-4 at 22 °C (Fig. 9D).

Similar cost function scenarios were observed at LT/EL, where *ambi* and *o:y* models fitted data best in Ct-1 and Oy-0 while model solution

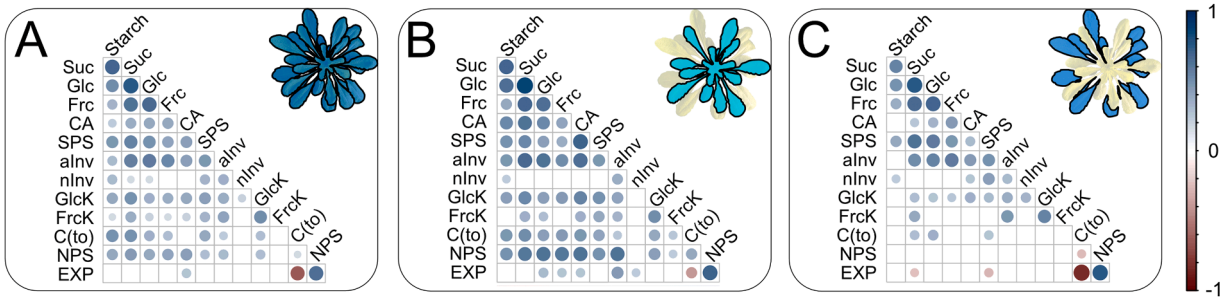

Fig. 8. Pearson correlation of metabolites, enzyme activities and estimated carbon fluxes in young and old leaf tissue. (A) Pearson correlation across all tissue, time points and accessions. (B) Pearson correlation across young tissue, time points and accessions. (C) Pearson correlation across old tissue, time points and accessions. The color bar indicates positive (blue) and negative (red) correlation coefficients. Blank fields: non-significant correlations ($p \geq 0.05$). Suc: sucrose; Glc: glucose; Frc: fructose; CA: carboxylic acids (i.e., summed citrate, malate and fumarate); SPS: sucrose phosphate synthase; aInv: acidic invertase; nInv: neutral invertase; GlK: glucokinase; FrK: fructokinase; C(to): carbon turnover rates; NPS: net photosynthesis rates; EXP: calculated export rates.

quality was indistinguishable in Rsch-4 (Fig. 9E, G, H). Hence, while all four tested model structures adequately captured the general diurnal dynamics of sucrose, glucose, and fructose concentrations in both young and old leaves under ambient and LT/HL conditions, the *ambi* and *o:y* assumptions yielded the most accurate representations of experimentally measured sucrose medians in old leaves (explicit solutions are shown in Supplementary Figs. S6–S9). Finally, however, the interpretation of model fitting in this study remains clearly limited by the low number of time points (eon, eod) which leaves considerable room for speculation about the dynamics during the day phase *in planta*.

Discussion

A combination of low air temperature and elevated light intensities represents an environment which many plant species might experience during their life cycle. For example, winter annuals which germinate in a relatively mild environment experience a significant temperature drop within the first weeks and months. In such an environment, plants need to quickly and efficiently adjust photosynthesis and metabolism to prevent a harmful disbalance of light energy absorption, photosynthetic electron transport, enzymatic CO_2 fixation and metabolism (Long et al., 1994). In the present study it was observed that *Arabidopsis* plants grown under short day conditions for eight to nine weeks show a gradient of F_v/F_m under LT/EL across the leaf rosette. This finding was conserved across the four tested natural accessions which originated both from northern and southern European habitats. Hence, although freezing tolerance was not explicitly tested here, this indicates that such a gradient is a conserved trait which appears both in putatively freezing sensitive and freezing tolerant accessions. Further analysis revealed that, even under ambient growth conditions, net CO_2 uptake rates varied significantly across the rosette, with older leaves exhibiting higher assimilation rates than younger ones. It remains speculation here, but the difference in net CO_2 uptake may result from a lowered leaf respiration rate which has been shown earlier to decrease with leaf expansion, maybe due to a lowered number of mitochondria per unit cell volume (Armstrong et al., 2006). Such a developmental shift in mitochondrially located rather than in photosynthetic processes might also explain why F_v/F_m did not differ between old and young tissue under ambient conditions. Interestingly, after exposure to LT/EL, both F_v/F_m and rates of NPS were found to be higher in young than in old tissue. Although all measurements were conducted at 22 °C and, hence, do not represent the situation in situ (i.e., 4 °C), this suggested that LT/EL induced a photosynthetic and metabolic adjustment which changed the physiological role of old and young leaves when compared to ambient conditions. This was further reflected in the amounts of starch and sucrose which were found to be highest at the end of the light period in young leaf tissue across all accessions. Across all accessions, diurnal dynamics of sucrose were more pronounced under LT/EL than under ambient conditions (see Fig. 5E-H). In contrast, old leaf tissue of Ct-1 and Fei-0 was found to have reduced starch dynamics while in Oy-0 and Rsch-4 both tissue types showed a significant starch accumulation during the day. This might hint towards differential capacities of starch accumulation in tissue of putatively cold sensitive (Ct-1, Fei-0) and cold tolerant (Oy-0, Rsch-4) accessions. However, also regulation of starch degradation might be differentially regulated in the two considered tissues which has been shown to play a critical role in the development of cold and freezing tolerance (Kaplan and Guy, 2005; Sicher, 2011; Nagler et al., 2015). Starch metabolism has been discussed frequently in context of abiotic stress response and acclimation capacity, sometimes also with different dynamics across species (Thalmann and Santelia, 2017). While it remains speculation here, maybe developmental differences in leaf tissue contribute to these reported discrepancies which might also have different consequences for different stressors. As starch remobilization plays an important role under diverse conditions, such developmental effects might also become critical for (metabolic) engineering and breeding strategies.

In a recent study it was shown on the level of transcripts and proteins that, under changing growth light intensities and temperature regimes, old leaves support development and growth of younger leaves (Luklova et al., 2025). While the authors of this study applied low light intensities in combination with cold treatment, which contrasts the stress scenario of the present study, they showed that freezing tolerance was associated with lipid metabolism, chloroplast number and size. Independent of the underlying molecular and cellular mechanisms, also in the present study, which applied elevated light instead of low light, evidence was provided for a supportive role of mature leaves for growth and development of immature, or young, leaves. Correlation analysis of metabolites, enzyme activities and diurnal carbon balance revealed that net photosynthesis positively correlates with LT/EL-induced dynamics of sugars, carboxylic acids and enzyme activities of the central carbohydrate metabolism. This suggests that, in young leaves, an increased carbon assimilation rate is reflected by increasing carbon pools, e.g. carbohydrates and carboxylic acids, which might result in a stimulation of enzymatic carbohydrate interconversion. This contrasts findings of a previous study which showed that (maximum) enzyme activities only weakly, or not at all, correlated with metabolite levels across a large panel of *Arabidopsis* accessions (Sulpice et al., 2010). However, in their study, the authors did not apply a cold and/or light stress which shows that the observed correlations might depend on the growth setup. Further, the present study provides compelling evidence for a differential correlation of enzymatic parameters, metabolites and carbon fluxes across one leaf rosette. For example, in old leaves, sucrose and the maximum activity of its biosynthesising enzyme SPS were found to negatively correlate with carbon export rates of the system, i.e., with the difference between input (NPS) and carbon turnover within the leaf. This was neither observed in a correlation analysis of young leaves nor

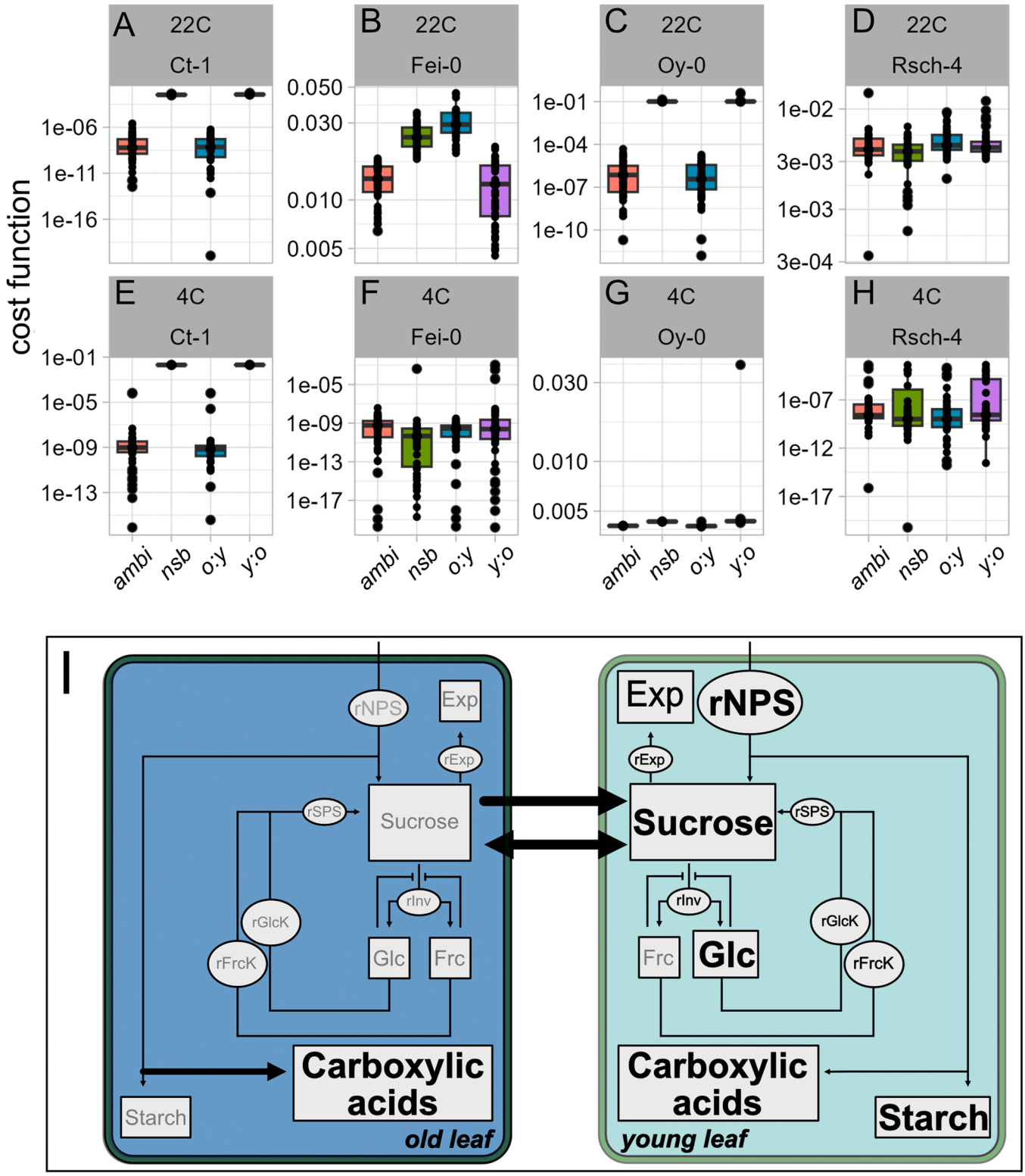

Fig. 9. Cost functions of optimized kinetic models to simulate putative sucrose fluxes between young and old leaf tissue. (A) – (D) Decadic logarithm of least squared errors (cost functions) for accessions at 22 °C, (E) – (H) Decadic logarithm of least squared errors (cost functions) for accessions at LT/EL (4C). Each model was optimized 50x. red: ambidirectional sucrose transport (*ambi*); green; no sucrose transport between tissues (*nsb*); blue: sucrose transport from old to young tissue (*o:y*); purple: sucrose transport from young to old tissue (*y:o*). (I) A graphical summary of the most dynamic metabolite pools and fluxes due to exposure to LT/EL. Increased font and arrow size indicates increased amounts and rates in a tissue type under LT/EL, respectively.

in a correlation analysis which did not discriminate between old and young tissue (see Fig. 8). This finding pointed towards a differential metabolic function of young and old leaf tissue when exposed to LT/EL. In general, young leaf tissue showed a strong increase of carbon uptake rates under LT/EL when compared to old tissue. But also, old leaf tissue stayed (at least) constant compared to ambient conditions. Hence, metabolic changes, e.g., lower starch and sugar levels could not be (purely) explained by a lowered photosynthetic carbon assimilation. Also, amounts of carboxylic acids determined in old leaf tissue were similar to amounts of young tissue after exposure to LT/EL which supports the hypothesis that different correlations resulted rather from differential metabolic regulation than from net photosynthetic limitations. Furthermore, young leaf tissue exhibited higher net CO_2 assimilation rates than old tissue following LT/EL exposure, whereas the opposite was observed under ambient conditions. Together with the simulation results of a kinetic model with putative sucrose exchange between old and young leaves, this pointed towards a changing role of carbon supply under LT/EL: the best simulations of experimental data were gained in models which allowed for a sucrose exchange between both tissues, and preferentially from old to young leaves.

The experimental verification of this finding remains difficult. One possible approach would be to use labelled CO_2, which could then be traced within the carbon metabolism. However, labelling would need to be applied specifically to old or young tissue, avoiding contamination of other tissue types. Additionally, genetic sensors could be employed, although these would first need to be established within the different genetic backgrounds of the natural accessions. Nevertheless, even though it remains a purely theoretical framework in the present study, the provided models may support the generation of hypotheses for future experiments.

While experimental and computational simulation results point towards dynamic sink-source relationships between both tissues under stress (Roitsch, 1999; Lemoine et al., 2013), the reason for such a dynamic remains elusive. Based on the finding that NPS rates in young leaf tissue can sufficiently supply and explain metabolite dynamics, even without sucrose exchange, it is hypothesised that the underlying plasticity of the metabolic system can equally well explain the observed metabolic phenotypes. Yet, as diurnal dynamics of most sugars under LT/EL were higher in young tissue than in old tissue, additional carbon import into the young metabolism could further improve the simulations.

Based on *in situ* stable isotope tracing it has previously been shown that sucrose utilization differs between *Arabidopsis* sink and source leaves (Dethloff et al., 2017). For example, citrate, fumarate and malate showed a higher label enrichment in sink than in source leaves. At least partially, this might also be reflected in the amounts of all three carboxylic acids quantified in the present study. Under ambient growth conditions, higher amounts of fumarate and malate were found in mature tissue than in young tissue (see Supplementary Figs. S3, S4). Compared to previous studies, however, only a minor diurnal accumulation was observed for fumarate (Dyson et al., 2016). Simultaneously, also the diurnal dynamics of sucrose were significantly lower in the present study than reported for Col-0 before (Dyson et al., 2016). This might indicate that diurnal accumulation rates of sugars and carboxylic acids represent specific traits across different natural accessions of *Arabidopsis thaliana*. This is supported by the finding that young tissue of Oy-0 and Rschew-4 showed a more pronounced accumulation of fumarate during the day than Ct-1 and Fei-0 at 22 °C (see Supplementary Fig. 3). Interestingly, under LT/EL, especially malate amounts became similar across accessions and tissues, except for Fei-0 where older tissue still had higher levels than young tissue. Without discriminating mature and immature leaf tissue, such environmentally induced dynamics within leaf rosettes would be hidden behind the total variance of experimental data. Hence, to reduce ambiguity and to improve interpretability of leaf metabolomes, separated tissue analysis in large leaf rosettes might be beneficial.

Finally, an obvious limitation of the present study is the low number of sampled time points across the light phase which reduces the discriminatory power between model simulation qualities, i.e., cost functions. However, together with the experimental data, the present study provides strong evidence for the need to separate *Arabidopsis* leaf rosettes in mature and immature parts if photosynthetic parameters, like F_v/F_m or CO_2 assimilation rates, indicate a gradient across leaf tissue. This might significantly improve interpretability and predictive power of quantitative models of metabolism which are developed to describe and predict plant growth, development and resilience in a changing environment.

Data availability statement

Data of this study is available in the supplements.

CRediT authorship contribution statement

Vladimir Brodsky: Writing – review & editing, Writing – original draft, Visualization, Validation, Supervision, Methodology, Investigation, Formal analysis, Data curation. **Anian Kerscher:** Investigation, Data curation. **Michaela Urban:** Investigation, Data curation. **Thomas Nägele:** Writing – review & editing, Writing – original draft, Visualization, Validation, Supervision, Software, Resources, Project administration, Methodology, Funding acquisition, Formal analysis, Data curation, Conceptualization.

Declaration of competing interest

The authors declare no conflict of interest.

Acknowledgements

We thank the members of Plant Evolutionary Cell Biology at LMU München and the members of AG Weckwerth at University of Vienna for fruitful discussions. Further, we thank the Graduate School Life Science Munich (LSM) for support. This work was funded by Deutsche Forschungsgemeinschaft (DFG), NA1545–5/1.

Supplementary materials

Supplementary material associated with this article can be found, in the online version, at doi:10.1016/j.stress.2025.100958.

References

Andrés, F., Kinoshita, A., Kalluri, N., Fernández, V., Falavigna, V.S., Cruz, T.M.D., Jang, S., Chiba, Y., Seo, M., Mettler-Altmann, T., Huettel, B., Coupland, G., 2020. The sugar transporter SWEET10 acts downstream of FLOWERING LOCUS T during floral transition of Arabidopsis thaliana. BMC Plant Biol. 20, 53.

Armstrong, A.F., Logan, D.C., Atkin, O.K., 2006. On the developmental dependence of leaf respiration: responses to short- and long-term changes in growth temperature. Am. J. Bot. 93, 1633–1639.

Bernier, G., Havelange, A., Houssa, C., Petitjean, A., Lejeune, P., 1993. Physiological signals that induce flowering. Plant Cell 5, 1147–1155.

Dethloff, F., Orf, I., Kopka, J., 2017. Rapid in situ 13C tracing of sucrose utilization in Arabidopsis sink and source leaves. Plant Methods 13, 87.

Durand, M., Mainson, D., Porcheron, B., Maurousset, L., Lemoine, R., Pourtau, N., 2018. Carbon source–sink relationship in *Arabidopsis thaliana*: the role of sucrose transporters. Planta 247, 587–611.

Dyson, B.C., Miller, M.A.E., Feil, R., Rattray, N., Bowsher, C.G., Goodacre, R., Lunn, J.E., Johnson, G.N., 2016. FUM2, a cytosolic fumarase, is essential for acclimation to low temperature in *Arabidopsis thaliana*. Plant Physiol. 172, 118–127.

Fürtauer, L., Nägele, T., 2016. Approximating the stabilization of cellular metabolism by compartmentalization. Theory Biosci. 135, 73–87.

Geigenberger, P., Stitt, M., 1991. A futile cycle of sucrose synthesis and degradation is involved regulating partitioning between sucrose starch and respiration in cotyledons of germinating ricinus-communis l. Seedlings when phloem transport is inhibited. Planta 185, 81–90.

Granot, D., David-Schwartz, R., Kelly, G., 2013. Hexose kinases and their role in sugar-sensing and plant development. Front. Plant Sci. 4, 44.

Kaplan, F., Guy, C.L., 2005. RNA interference of Arabidopsis beta-amylase8 prevents maltose accumulation upon cold shock and increases sensitivity of PSII photochemical efficiency to freezing stress. Plant J. 44, 730–743.
Kitashova, A., Adler, S.O., Richter, A.S., Eberlein, S., Dziubek, D., Klipp, E., Nägele, T., 2023. Limitation of sucrose biosynthesis shapes carbon partitioning during plant cold acclimation. Plant Cell Environ. 46, 464–478.
Koch, K., 2004. Sucrose metabolism: regulatory mechanisms and pivotal roles in sugar sensing and plant development. Curr. Opin. Plant Biol. 7, 235–246.
Lemoine, R., La Camera, S., Atanassova, R., Dedaldechamp, F., Allario, T., Pourtau, N., Bonnemain, J.L., Laloi, M., Coutos-Thevenot, P., Maurousset, L., Faucher, M., Girousse, C., Lemonnier, P., Parrilla, J., Durand, M., 2013. Source-to-sink transport of sugar and regulation by environmental factors. Front. Plant Sci. 4, 272.
Long, S., Humphries, S., Falkowski, P., 1994. Photoinhibition of photosynthesis in nature. Annu. Rev. Plant Physiol. Plant Mol. Biol. 45, 633–662.
Luklova, M., Dubois, M., Kameniarova, M., Plackova, K., Novak, J., Kopecka, R., Karady, M., Pavlu, J., Skalak, J., Jindal, S., Tubic, L., Quddoos, Z., Novak, O., Inze, D., Cerny, M., 2025. Light quantity impacts early response to cold and cold acclimation in young leaves of Arabidopsis. Plant Cell Environ. https://doi.org/10.1111/pce.15481.
Moore, B., Zhou, L., Rolland, F., Hall, Q., Cheng, W.H., Liu, Y.X., Hwang, I., Jones, T., Sheen, J., 2003. Role of the Arabidopsis glucose sensor HXK1 in nutrient, light, and hormonal signaling. Science 300, 332–336 (1979).
Nägele, T., 2022. Metabolic regulation of subcellular sucrose cleavage inferred from quantitative analysis of metabolic functions. Quant. Plant Biol. 3, e10.
Nägele, T., Henkel, S., Hörmiller, I., Sauter, T., Sawodny, O., Ederer, M., Heyer, A.G., 2010. Mathematical modeling of the central carbohydrate metabolism in Arabidopsis reveals a substantial regulatory influence of vacuolar invertase on whole plant carbon metabolism. Plant Physiol. 153, 260–272.
Nägele, T., Heyer, A.G., 2013. Approximating subcellular organisation of carbohydrate metabolism during cold acclimation in different natural accessions of *Arabidopsis thaliana*. New Phytol. 198, 777–787.
Nägele, T., Kandel, B.A., Frana, S., Meißner, M., Heyer, A.G., 2011. A systems biology approach for the analysis of carbohydrate dynamics during acclimation to low temperature in *Arabidopsis thaliana*. FEBS J. 278, 506–518.
Nägele, T., Stutz, S., Hörmiller, I.I., Heyer, A.G., 2012. Identification of a metabolic bottleneck for cold acclimation in *Arabidopsis thaliana*. Plant J. 72, 102–114.
Nagler, M., Nukarinen, E., Weckwerth, W., Nägele, T., 2015. Integrative molecular profiling indicates a central role of transitory starch breakdown in establishing a stable C/N homeostasis during cold acclimation in two natural accessions of *Arabidopsis thaliana*. BMC Plant Biol. 15, 284.
Rasmussen, S., Barah, P., Suarez-Rodriguez, M.C., Bressendorff, S., Friis, P., Costantino, P., Bones, A.M., Nielsen, H.B., Mundy, J., 2013. Transcriptome responses to combinations of stresses in Arabidopsis. Plant Physiol. 161, 1783–1794.
Roitsch, T., 1999. Source-sink regulation by sugar and stress. Curr. Opin. Plant Biol. 2, 198–206.
Roitsch, T., González, M.C., 2004. Function and regulation of plant invertases: sweet sensations. Trends Plant Sci. 9, 606–613.
Rolland, F., Baena-Gonzalez, E., Sheen, J., 2006. Sugar sensing and signaling in plants: conserved and novel mechanisms. Annu. Rev. Plant Biol. 57, 675–709.
Ruan, Y.L., 2014. Sucrose metabolism: gateway to diverse carbon use and sugar signaling. Annu. Rev. Plant Biol. 65, 33–67.
Ruan, Y.L., Jin, Y., Yang, Y.J., Li, G.J., Boyer, J.S., 2010. Sugar input, metabolism, and signaling mediated by invertase: roles in development, yield potential, and response to drought and heat. Mol. Plant 3, 942–955.
Shaar-Moshe, L., Hayouka, R., Roessner, U., Peleg, Z., 2019. Phenotypic and metabolic plasticity shapes life-history strategies under combinations of abiotic stresses. Plant Direct 3, e00113.
Shi, H., Schwender, J., 2016. Mathematical models of plant metabolism. Curr. Opin. Biotechnol. 37, 143–152.
Sicher, R., 2011. Carbon partitioning and the impact of starch deficiency on the initial response of Arabidopsis to chilling temperatures. Plant Sci. 181, 167–176.
Stelling, J., Klamt, S., Bettenbrock, K., Schuster, S., Gilles, E.D., 2002. Metabolic network structure determines key aspects of functionality and regulation. Nature 420, 190–193.
Strand, A., Foyer, C.H., Gustafsson, P., Gardestrom, P., Hurry, V., 2003. Altering flux through the sucrose biosynthesis pathway in transgenic *Arabidopsis thaliana* modifies photosynthetic acclimation at low temperatures and the development of freezing tolerance. Plant Cell Environ. 26, 523–535.
Sturm, A., 1999. Invertases. Primary structures, functions, and roles in plant development and sucrose partitioning. Plant Physiol. 121, 1–8.
Sulpice, R., Trenkamp, S., Steinfath, M., Usadel, B., Gibon, Y., Witucka-Wall, H., Pyl, E. T., Tschoep, H., Steinhauser, M.C., Guenther, M., Hoehne, M., Rohwer, J.M., Altmann, T., Fernie, A.R., Stitt, M., 2010. Network analysis of enzyme activities and metabolite levels and their relationship to biomass in a large panel of Arabidopsis accessions. Plant Cell 22, 2872–2893.
Thalmann, M., Santelia, D., 2017. Starch as a determinant of plant fitness under abiotic stress. New Phytol. 214, 943–951.
Töpfer, N., Braam, T., Shameer, S., Ratcliffe, R.G., Sweetlove, L.J., 2020. Alternative crassulacean acid metabolism modes provide environment-specific water-saving benefits in a leaf metabolic model. Plant Cell 32, 3689–3705.
Vaz, A.I.F., Vicente, L.N., 2007. A particle swarm pattern search method for bound constrained global optimization. J. Glob. Optim. 39, 197–219.
Yano, R., Nakamura, M., Yoneyama, T., Nishida, I., 2005. Starch-related alpha-glucan/water dikinase is involved in the cold-induced development of freezing tolerance in Arabidopsis. Plant Physiol. 138, 837–846.
Yu, S., Cao, L., Zhou, C.M., Zhang, T.Q., Lian, H., Sun, Y., Wu, J., Huang, J., Wang, G., Wang, J.W., 2013. Sugar is an endogenous cue for juvenile-to-adult phase transition in plants. Elife 2, e00269.